

## OPTICAL PROPERTIES OF LEAD IN THE VISIBLE AND INFRARED SPECTRAL RANGES

A. I. GOLOVASHKIN and G. P. MOTULEVICH

P. N. Lebedev Physics Institute, Academy of Sciences, U.S.S.R.

Submitted May 30, 1967

Zh. Eksp. Teor. Fiz. 53, 1526--1538 (November, 1967)

The optical properties of lead are measured in the spectral range from 0.48 to 2.76 eV at  $T = 293$  and  $78^\circ\text{K}$  and in the range 0.48--2.3 eV at  $T = 4.2^\circ\text{K}$ . The contribution of interband transitions to the dielectric constant and conductivity of lead is determined. Two conductivity bands are found which are identified with bands caused by Fourier components of the pseudopotential. Fourier components of the pseudopotentials  $V_{111}$  and  $V_{200}$  are determined at the three indicated temperatures. The calculated and experimental maximum values of the interband conductivity for both bands are compared and good agreement is observed between theory and the experiments. Electron conductivity parameters such as electron concentration, area of the Fermi surface, and mean velocity on the Fermi surface are determined from the values of the Fourier components of the pseudopotential. These values of the parameters are compared with those obtained from measurements in the long-wave region. The agreement is found to be satisfactory. The temperature dependence of the main electron characteristics of lead is determined.

## INTRODUCTION

THE concentration of conduction electrons in lead is considerably lower than that of valence electrons. This is apparently true for all multivalent metals; at least, all metals studied by optical methods confirm this conclusion. As has recently been shown,<sup>[1,2]</sup> this is basically related to the influence of the periodic lattice potential. A relation connecting  $N_{\text{opt}}$  with the Fourier components of the pseudopotential  $V_g$  ( $N_{\text{opt}}$  is the concentration of conduction electrons determined by optical methods) has been obtained in<sup>[1]</sup>. As has been shown in<sup>[3]</sup>, these Fourier components can in turn be determined from optical measurements. Detailed measurements of the optical constants in the visible and near infrared regions of the spectrum are essential for this purpose. In this work such measurements have been carried out for lead. The measurements were carried out at helium, nitrogen, and room temperatures. In conjunction with the results of our previous work,<sup>[4]</sup> the results obtained made it possible to determine the main electron characteristics of lead and their temperature dependence.

## EXPERIMENTAL PART

1. A setup, the schematic diagram of whose optics is shown in Fig. 1<sup>1)</sup>, was used to measure the optical constants.

As the dispersive system we used a monochromator with glass optics. The detectors were a FÉU-28 photomultiplier for the 0.45--1.2  $\mu$  range and a FSA-1 photoresistor for the 0.8--2.6  $\mu$  range. The null method of measuring the optical constants made it possible to employ a dc arc as the light source.

Polaroids served as polarizers in the 0.45--0.74  $\mu$  spectral range and selenium films in the 0.70--2.6  $\mu$  range. A special investigation of the characteristics of

the employed polarizers was carried out. In the indicated spectral range the polaroids had an intensity ratio of useful to parasitic light components of 7000 in the 0.5--0.72  $\mu$  region, and of more than 1000 at the limits of their useful range. Their transmission was 45 percent in the main portion of the indicated spectral range and decreased to 20 percent at  $\lambda = 0.45 \mu$ . The corresponding characteristics of the selenium polarizers were: a ratio of the useful and parasitic components of no less than 500, and a transmission of 40 percent.

The Soleil-Babinet type quartz compensator used made it possible to measure the phase difference between the p and s components with an accuracy of 2'.

Fourfold and eightfold reflection of the investigated mirrors was used to measure the optical constants  $n$  and  $\kappa$  ( $n - i\kappa$  is the complex refractive index). With the aid of the compensator the phase difference was made to equal an odd multiple of  $\pi/2$ , and the amplitudes of the p and s components were equalized by means of the analyzer. The phase difference  $\Delta$  and the azimuth  $\rho$  obtained in this fashion were basically determined by the investigated mirrors. However, all the elements of the setup located before the analyzer A (mainly the mirrors  $L_1$  and  $L_2$ ) could make a small contribution to these values. The parasitic phase and azimuth shift was specially measured for each wavelength. For this purpose  $\Delta$  and  $\rho$  were measured without the investigated mirrors. Such measurements made it possible to determine the

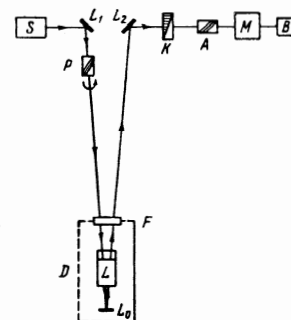


FIG. 1. Optical diagram of the setup. S—illuminator producing a parallel beam of light;  $L_1$ ,  $L_2$ , and  $L_0$ —flat mirrors; L—investigated mirrors; P—rotating polarizer; A—analyzer, K—compensator, M—monochromator; B—radiation detector; F—window; D—low-temperature part.

<sup>1)</sup>The principle of the setup and the method of measurement have been described previously. [5-6]

phase and azimuth shift connected solely with the mirrors being investigated. The correction due to the effect of the remaining parts of the setup, other than the investigated mirrors, on the polarization of the light was small. It amounted to 5–6 percent in the case of  $\Delta$  with four reflections from the investigated mirrors; for eight reflections it was less than 2 percent. The  $\tan \rho$  correction amounted in both instances to less than 1 percent in the 1–2.6  $\mu$  range and 2–6 percent in the remaining range. In the narrow spectral range corresponding to the reflection minimum from the aluminum mirrors (0.8–0.85  $\mu$ ) the correction reached up to 9 percent.

In the spectral range in which a sharp conductivity maximum  $\sigma(\lambda)$  occurs, the optical constants were measured in steps of 0.01  $\mu$ . The spectral width of the slit amounted in this region to 0.01–0.02  $\mu$ . In the region in which the second singularity of  $\sigma(\lambda)$  was observed, the measurements were carried out in steps of 0.02–0.05  $\mu$ . The spectral width of the slit in this range was 0.02–0.05  $\mu$ . In the region of longer wavelengths the measurements were carried out in steps of 0.1  $\mu$  and the spectral width of the slit was 0.1  $\mu$ . At the very end of the investigated range the spectral width of the slit was 0.2  $\mu$ .

The low-temperature part of the setup was the same as in [5]. The measurements were carried out at three temperatures: 293, 78, and 4.2°K. The temperature of the investigated mirrors was controlled during the measurement of the optical constants. At 4.2°K the

temperature at the beginning and at the end of the experiment differed by 0.02°. The measurements of the optical constants were carried out in the following sequence: first, directly after the samples were prepared, the optical constants were measured at room temperature; they were then measured at nitrogen and helium temperature. Special experiments were conducted to establish the effect of the possible oxidation of the samples. To this end the optical constants were measured both immediately after the preparation of the samples and after some time. Keeping the samples in the cryostat for 24 hours did not change the optical constants; small changes (2–3 percent for  $n$  and 1–2 percent for  $\kappa$ ) were only observed after four days. This indicates that good lead mirror surfaces oxidize rather slowly, so that the results of our measurements are practically unaffected by oxidation.

2. The samples were prepared by evaporating 99.999 percent pure lead in a  $(2-5) \times 10^{-6}$  mm Hg vacuum from tantalum boats onto polished glass substrates which were in addition cleaned by a gas discharge in a  $10^{-1}-10^{-2}$  mm Hg vacuum. The rate of deposition was  $\sim 500$  Å/sec. As in [4], the static characteristics of the films coincided with those of the bulk metal. The residual resistivity of the films used was even smaller than for the films in [4], and amounted to  $< 0.3$  percent of the resistivity at room temperature. The residual resistivity of the films used both in this work and in [4] has practically no effect on the optical constants, even at helium temperatures.

Table I. Optical constants of lead

$\lambda$	T = 293° K		T = 78° K		T = 4.2° K		$\lambda$	T = 293° K		T = 78° K		T = 4.2° K		
	n	$\kappa$	n	$\kappa$	n	$\kappa$		n	$\kappa$	n	$\kappa$	n	$\kappa$	
0.45	1.44 <sub>5</sub>	3.18	1.56	3.20	—	—	0.88	1.41	4.56	1.01	4.25	0.940	4.16	
0.46	1.54 <sub>5</sub>	3.20	1.57 <sub>5</sub>	3.22	—	—	0.90	1.40	4.68	0.983	4.37	0.904	4.27	
0.47	1.58	3.23	1.64	3.22	—	—	0.92	1.38 <sub>5</sub>	4.80	0.956	4.49	0.870	4.39	
0.48	1.62	3.25	1.65	3.22	—	—	—	0.95	1.38 <sub>5</sub>	4.99	0.917	4.67	0.821	4.57
0.49	1.68	3.28	1.65 <sub>5</sub>	3.22	—	—	0.98	1.38	5.16	0.878	4.86	0.771	4.76	
0.50	1.70 <sub>5</sub>	3.30	1.67 <sub>5</sub>	3.24	—	—	1.00	1.38	5.32	0.845	5.00	0.721	4.90	
0.51	1.74	3.31	1.68 <sub>5</sub>	3.27	—	—	1.05	1.38 <sub>5</sub>	5.62	0.801	5.30	0.656	5.22	
0.52	1.75 <sub>5</sub>	3.34	1.70	3.31	—	—	1.10	1.40	5.98	0.743	5.63	0.574	5.58	
0.53	1.78 <sub>5</sub>	3.36	1.73	3.35	—	—	1.15	1.41 <sub>5</sub>	6.31	0.678	6.00	0.485	5.92	
0.54	1.81	3.37	1.78	3.39	1.82	3.46	1.20	1.44 <sub>5</sub>	6.59	0.651	6.28	0.417	6.29	
0.55	1.83 <sub>5</sub>	3.40	1.82 <sub>5</sub>	3.43	1.88 <sub>5</sub>	3.50	1.25	1.48 <sub>5</sub>	6.93	0.599	6.66	0.346	6.66	
0.56	1.87	3.41	1.87 <sub>5</sub>	3.45	1.97	3.51	1.30	1.50	7.23	0.583	6.96	0.312	6.96	
0.57	1.87	3.43	1.91	3.46	2.04	3.52	1.35	1.52 <sub>5</sub>	7.48	—	—	0.294	7.26	
0.58	1.90	3.43	1.96 <sub>5</sub>	3.47	2.11	3.52	1.40	1.58	7.74	0.566	7.59	0.285	7.59	
0.59	1.91	3.44	2.01	3.46	2.17	3.52	1.45	1.60	8.01	—	—	0.290	7.90	
0.60	1.91 <sub>5</sub>	3.45	2.06	3.44	2.26	3.50	1.50	1.64 <sub>5</sub>	8.30	0.575	8.23	0.275	8.24	
0.61	1.94 <sub>5</sub>	3.46	2.10	3.42	2.29	3.45	1.55	1.69 <sub>5</sub>	8.58	—	—	—	—	
0.62	1.94 <sub>5</sub>	3.47	2.11	3.38	2.34	3.38	1.60	1.77 <sub>5</sub>	8.90	0.611	8.93	0.300	8.94	
0.63	1.95	3.48	2.14	3.34	2.39	3.27	1.70	1.89 <sub>5</sub>	9.47	0.647	9.59	0.312	9.57	
0.64	1.94 <sub>5</sub>	3.49	2.13	3.28	2.39	3.16	1.80	2.05	10.1 <sub>5</sub>	0.683	10.2	0.336	10.3 <sub>5</sub>	
0.65	1.91 <sub>5</sub>	3.51	2.09	3.25	2.34	3.09	1.90	2.18	10.7	0.728	10.8	0.338	11.0	
0.66	1.89 <sub>5</sub>	3.51	2.08	3.19	2.28	3.02	2.00	2.32	11.2	0.783	11.3 <sub>5</sub>	0.387	11.5 <sub>5</sub>	
0.67	—	—	2.02	3.14	2.18	2.93	2.10	2.47	11.7 <sub>5</sub>	0.835	11.9 <sub>5</sub>	0.382	12.1	
0.68	1.85 <sub>5</sub>	3.53	1.96 <sub>5</sub>	3.10	2.09	2.89	2.20	2.63	12.2	0.901	12.5 <sub>5</sub>	0.448	12.7 <sub>5</sub>	
0.69	—	—	1.88	3.08	1.97	2.84	2.30	2.84	12.8	0.949	13.1 <sub>5</sub>	0.409	13.3	
0.70	1.78 <sub>5</sub>	3.57	1.80	3.07	1.85	2.82	2.40	3.03	13.2	0.997	13.7 <sub>5</sub>	0.541	13.9 <sub>5</sub>	
0.71	—	—	1.68 <sub>5</sub>	3.08	1.67 <sub>5</sub>	2.83	2.50	3.22	13.9	1.05	14.3	0.586	14.5 <sub>5</sub>	
0.72	1.71	3.64	1.58	3.13	1.54 <sub>5</sub>	2.89	2.55	3.34	14.1 <sub>5</sub>	—	—	0.597	14.7 <sub>5</sub>	
0.73	—	—	1.47 <sub>5</sub>	3.17	1.40	2.97	2.60	3.45	14.4 <sub>5</sub>	1.19 <sub>5</sub>	14.8 <sub>5</sub>	0.614	15.0 <sub>5</sub>	
0.74	1.63 <sub>5</sub>	3.73	1.39	3.24	1.30 <sub>5</sub>	3.06	3.0	4.27	16.4	1.53	17.3	0.81	17.3	
0.75	1.60	3.78	1.34	3.33	1.24	3.15	3.5	5.39	18.6	2.01	20.4	1.10	20.1	
0.76	1.57	3.84	1.28	3.41	1.17 <sub>5</sub>	3.26	4.0	6.58	20.8	2.48	22.9	1.49	23.1	
0.78	1.52 <sub>5</sub>	3.96	1.18 <sub>5</sub>	3.58	1.09	3.46	5.0	9.04	24.8	3.99	28.7	2.15	28.6	
0.79	—	—	1.16 <sub>5</sub>	3.65	1.07	3.58	6.0	11.7	28.1	5.41	33.9	2.95	34.4	
0.80	1.50 <sub>5</sub>	4.09	1.13	3.73	1.04	3.61	7.0	14.1	30.9	7.16	38.7	3.75	39.9	
0.81	—	—	—	—	1.02 <sub>5</sub>	3.75	8.0	16.4	33.6	8.82	43.9	4.50	45.5	
0.82	1.47	4.18	1.09	3.86	1.00 <sub>5</sub>	3.78	9.0	18.7	35.8	10.5	49.1	5.56	50.6	
0.84	—	—	—	—	0.989	3.92	10.0	21.0	37.4	12.3	54.4	6.70	55.9	
0.85	1.44	4.35	1.05 <sub>5</sub>	4.05	0.976	3.97	11.0	23.2	39.2	14.4	59.1	7.90	61.3	
0.86	—	—	—	—	0.965	4.04	12.0	24.6	40.5	16.3	63.5	9.20	66.5	

Here  $\lambda$  is the wavelength of the light in microns.

**Table II.** The results of processing of the optical constants of lead in accordance with the formulas of the weakly anomalous skin effect

$\lambda$	$N_{\text{opt}} \cdot 10^{-23}$	$v \cdot 10^{-14}$	$v_F \cdot 10^{-8}$	$\beta_1 \cdot 10^4$	$\beta_2 \cdot 10^4$	$\lambda$	$N_{\text{opt}} \cdot 10^{-23}$	$v \cdot 10^{-14}$	$v_F \cdot 10^{-8}$	$\beta_1 \cdot 10^4$	$\beta_2 \cdot 10^4$
$T = 293^\circ \text{K}$											
12.0	3.89	3.04	0.99	3.0	2.6	2.40	3.72	1.01	0.97	0.09	11.4
11.0	4.09	3.13	1.01	2.9	2.7	2.30	3.71	1.06	0.96	0.09	11.0
10.0	4.05	3.08	1.01	2.6	2.9	2.20	3.69	1.11	0.96	0.09	10.5
9.0	4.02	2.98	1.00	2.3	3.2	2.10	3.67	1.13	0.96	0.08	10.2
8.0	4.04	2.98	1.01	2.1	3.3	2.00	3.65	1.18	0.96	0.08	9.8
7.0	4.08	3.05	1.01	1.8	3.4	1.90	3.65	1.21	0.96	0.07	9.6
6.0	4.13	3.09	1.02	1.5	3.6	1.80	3.63	1.28	0.96	0.07	9.1
5.0	4.11	3.08	1.02	1.1	3.8	1.70	3.60	1.38	0.96	0.06	8.4
4.0	4.09	3.21	1.01	0.80	3.8	1.60	3.52	1.50	0.94	0.06	7.7
3.5	4.07	3.30	1.01	0.85	3.8	1.50	3.41	1.64	0.92	0.06	6.8
3.0	4.10	3.39	1.01	0.52	3.8						
2.60	4.10	3.55	1.01	0.42	3.7						
2.55	4.07	3.57	1.01	0.40	3.6						
2.50	4.06	3.57	1.01	0.39	3.6						
2.40	3.96	3.69	1.00	0.37	3.4						
2.30	4.01	3.70	1.00	0.34	3.5						
2.20	3.95	3.75	1.00	0.31	3.4						
2.10	3.99	3.82	1.00	0.29	3.4						
2.00	3.98	3.95	1.00	0.28	3.3						
1.90	4.01	4.09	1.00	0.26	3.2						
1.80	4.01	4.28	1.00	0.25	3.0						
1.70	3.91	4.50	0.99	0.22	2.8						
1.60	3.89	4.77	0.99	0.21	2.7						
1.55	3.85	4.88	0.98	0.20	2.7						
1.50	3.84	5.06	0.98	0.19	2.5						
$T = 78^\circ \text{K}$											
12.0	3.86	0.746	0.98	1.6	14.9						
11.0	3.90	0.768	0.99	1.4	14.7						
10.0	3.89	0.776	0.99	1.2	14.6						
9.0	3.84	0.816	0.98	1.0	13.9						
8.0	3.82	0.863	0.98	0.85	13.2						
7.0	3.80	0.907	0.98	0.69	12.6						
6.0	3.86	0.900	0.98	0.52	13.0						
5.0	3.91	0.936	0.99	0.38	12.7						
4.0	3.79	0.901	0.98	0.23	12.8						
3.5	3.91	0.936	0.99	0.19	12.8						
3.0	3.80	0.987	0.98	0.14	11.9						
2.60	3.71	1.04	0.97	0.11	11.1						
2.50	3.71	0.983	0.97	0.10	11.7						
$T = 4,2^\circ \text{K}$											
12.0	3.64	0.316	0.96	0.50	28.9						
11.0	3.66	0.322	0.96	0.43	28.6						
10.0	3.65	0.331	0.96	0.37	28.0						
9.0	3.67	0.338	0.96	0.31	27.7						
8.0	3.72	0.340	0.97	0.25	27.9						
7.0	3.73	0.380	0.97	0.23	25.7						
6.0	3.75	0.411	0.97	0.19	24.4						
5.0	3.72	0.439	0.97	0.14	23.0						
4.0	3.77	0.478	0.97	0.10	21.8						
3.5	3.71	0.460	0.97	0.07	22.2						
3.0	3.73	0.458	0.97	0.05	22.4						
2.60	3.76	0.460	0.97	0.04	22.4						
2.55	3.75	0.467	0.97	0.04	22.1						
2.50	3.80	0.474	0.98	0.04	22.1						
2.40	3.79	0.476	0.97	0.04	21.9						
2.30	3.74	0.372	0.97	0.02	26.2						
2.20	3.76	0.470	0.97	0.03	22.0						
2.10	3.71	0.436	0.97	0.02	23.1						
2.00	3.73	0.500	0.97	0.03	20.9						
1.90	3.75	0.477	0.97	0.02	21.7						
1.80	3.70	0.550	0.96	0.02	19.2						
1.70	3.55	0.598	0.94	0.02	17.3						
1.60	3.49	0.668	0.94	0.02	15.6						
1.50	3.38	0.720	0.92	0.02	14.2						

Here  $N_{\text{opt}}$  is in  $\text{cm}^{-3}$ ,  $v$  in  $\text{sec}^{-1}$ ,  $v_F$  in  $\text{cm/sec}$ , and  $\lambda$  in microns.

## RESULTS OF MEASUREMENTS

In order to increase the accuracy of the results, we carried out many series of measurements of  $n$  and  $\kappa$  at all three temperatures. Each series of measurements was carried out on newly prepared samples. The final results were obtained by averaging over all series. They are given in Table I. A comparison shows that in the range in which they overlap the results of this work coincide with the results of our previous work.<sup>[4]</sup> Taking into account this fact, we present in Table I the values of the optical constants obtained in<sup>[4]</sup> for the range 3–12  $\mu$ .

The error in the determination of the optical constants amounted at room temperature to 1.5–2 percent in  $n$  and 1–1.5 percent in  $\kappa$ ; at nitrogen and helium temperatures the error in  $n$  amounted to 1.5–2 percent in the principal spectral range and 2–5 percent at its long-wave limit, and for  $\kappa$  it amounted to 0.5–1 percent over the entire range. The indicated error was determined from the scatter of the data in different series. The error in the measurements of  $n$  and  $\kappa$  within a single series was even smaller.

It is seen from Table I that there is a sharp maximum of  $n(\lambda)$  in the region of 0.63–0.64  $\mu$ . Its magnitude and width are temperature dependent. It becomes sharpest at helium temperatures. In addition to this main maximum on the curve that describes the  $n(\lambda)$  dependence, there is also a clearly manifested singularity in the

region of 0.8–1.5  $\mu$ . This singularity is manifested most clearly at helium temperatures, but it also appears at room temperature. The same singularities appear in the  $\kappa(\lambda)$  dependence in the same spectral regions as in the  $n(\lambda)$  dependence, but they are manifested much more weakly.

## TREATMENT OF EXPERIMENTAL RESULTS

1. In order to separate the contribution of interband transitions to the dielectric constant  $\epsilon$  and the conductivity  $\sigma$ , one must determine the basic characteristics of the conduction electrons. The latter can be obtained from the results of measurements in the long-wave region. A weakly anomalous skin effect occurs in lead at all temperatures. The treatment was therefore in accordance with formulas (1)–(7) presented in<sup>[2]</sup>. The results are given in Table II<sup>2)</sup>. The following micro-characteristics calculated for various wavelengths  $\lambda$  are presented in this table: the concentration of conduction electrons  $N_{\text{opt}}$ , the collision frequency of the electrons  $\nu$ , the average velocity of the electrons on the Fermi surface  $v_F$ , and the corrections  $\beta_1$  and  $\beta_2$  connected with the anomalous nature of the skin effect.

The values of the corrections  $\beta_1$  and  $\beta_2$  are small

<sup>2)</sup>In [4] we have also used the formulas of the weakly anomalous skin effect: however, the mean velocity of the electrons on the Fermi surface was determined by a less accurate method.

Table III. The microcharacteristics of lead

	$T = 293^\circ \text{K}$	$T = 78^\circ \text{K}$	$T = 4.2^\circ \text{K}$
$N_a \cdot 10^{-22}$	3,29	3,34	3,36
$N_{\text{opt}} \cdot 10^{-23}$	4,06	3,85	3,73
$N_{\text{opt}}/N_a$	1,23	1,15	1,11
$v_F \cdot 10^{-8}$	1,01	0,98	0,97
$\nu \cdot 10^{-14}$	3,07	0,87	0,41
$S_F \cdot 10^{17}$	2,00	1,88	1,85
$\beta_2 \cdot 10^2$	3,4	13	24
$(\beta_1/\lambda^2) \cdot 10^4$	4,0	1,4	0,5

The concentrations of  $N_a$  and  $N_{\text{opt}}$  are given in  $\text{cm}^{-3}$ ,  $S_F$  in  $\text{g}^2 \cdot \text{cm}^{-2} \cdot \text{sec}^{-2}$ ,  $v_F$  in  $\text{cm}/\text{sec}$ ,  $\nu$  in  $\text{sec}^{-1}$ , and  $\lambda$  in microns.

compared with unity, a fact which indicates that the formulas for the weakly anomalous skin effect are applicable. At the same time, the use of the formulas of the normal skin effect leads to large errors, particularly at low temperatures for which  $\beta_2$  reaches values  $\sim 0.25$ .

The data of Table II allow one to find a spectral range within which the above characteristics are determined solely by the conduction electrons. This range was  $2.5\text{--}12 \mu$  for  $T = 293^\circ \text{K}$ ,  $3\text{--}12 \mu$  for  $T = 78^\circ \text{K}$ , and  $1.8\text{--}12 \mu$  for  $T = 4.2^\circ \text{K}$ . The average values of  $N_{\text{opt}}$ ,  $v_F$ ,  $\beta_1/\lambda^2$  and  $\beta_2$  obtained in these ranges are presented in Table III. The value of  $\nu$  is more sensitive to interband transitions than  $N_{\text{opt}}$ ; the spectral ranges for which the average values of  $\nu$  were obtained were therefore somewhat smaller. They were:  $4\text{--}12 \mu$  for  $T = 293^\circ \text{K}$ ,  $3\text{--}12 \mu$  for  $T = 78^\circ \text{K}$ , and  $2\text{--}12 \mu$  for  $T = 4.2^\circ \text{K}$ . The average values of  $\nu$  are also presented in Table III, which also includes values of the total area  $S_F$  of the Fermi surface obtained in accordance with formula (7) of [2].

The error in the determination of the average values of the microcharacteristics of lead was obtained from the scatter of the data referring to different wavelengths; it amounted to 1 percent for  $N_{\text{opt}}$ , 1–4 percent for  $\nu$ , 6–10 percent for  $\beta_2$ , and 10–30 percent for  $\beta_1/\lambda^2$ . The error in the average value of  $v_F$  is not determined by the scatter of the data referring to different  $\lambda$  but by the accuracy of the employed formulas. It amounts to several percent.

In determining the temperature dependence of the value of  $N_a$  of lead we made use of the temperature dependence of the density obtained by White.<sup>[7]</sup>

The average values given in Table III were used in determining the contribution of the conduction electrons to the complex dielectric constant  $\epsilon' = \epsilon - i(4\pi\sigma/\omega)$  in the visible and near infrared region of the spectrum.

2. In determining the effect of interband transitions on the optical constants we took into account the additivity of the dielectric constant  $\epsilon$  and of the conductivity  $\sigma$ , i.e., we assumed that

$$\epsilon = \epsilon_e + \tilde{\epsilon}, \quad (1)$$

$$\sigma = \sigma_e + \tilde{\sigma}. \quad (2)$$

Here  $\tilde{\epsilon}$  and  $\tilde{\sigma}$  refer to interband transitions, and  $\epsilon_e$  and  $\sigma_e$  to the conduction electrons.

The values of  $\epsilon_e$  and  $\sigma_e$  were determined from the formulas obtained for the case of the weak anomalous skin effect

$$\epsilon_e = - \left( \frac{4\pi e^2}{m} N_{\text{opt}} \right) \frac{1}{\omega^2 + \nu^2} (1 - B_1), \quad (3)$$

$$B_1 = \beta_1 + \frac{2\nu^2}{\omega^2 + \nu^2} (\beta_2 - \beta_1), \quad (4)$$

$$\sigma_e = \left( \frac{e^2}{m} N_{\text{opt}} \right) \frac{\nu}{\omega^2 + \nu^2} (1 - B_2), \quad (5)$$

$$B_2 = \beta_2 + \frac{2\omega^2}{\omega^2 + \nu^2} (\beta_1 - \beta_2). \quad (6)$$

The notation in these formulas coincides with that in [2]. In these formulas we have confined ourselves to the first order in the corrections  $\beta_1$  and  $\beta_2$  connected with the anomalous nature of the skin effect.

As follows from these formulas and from Table III, the value of  $\beta_1$  has practically no effect on  $\epsilon_e$  and  $\sigma_e$  in the visible and near infrared ranges. Account of the coefficient  $\beta_2$  is essential.

Making use of the results of Table I and of Eqs. (1)–(6), one can readily calculate  $\epsilon$  and  $\tilde{\sigma}$ . The separation of  $\tilde{\sigma}$  at all temperatures is carried out with good accuracy because the contribution of the conduction electrons in the region  $\hbar\omega = 2 \text{ eV}$  is between 1 percent at helium temperature and 10 percent at room temperature, and in the region of 1.5 eV from 6 percent at helium temperature up to 20 percent at room temperature. The obtained values of  $\tilde{\sigma}$  are given in Figs. 2–4.

Figures 2–4 show that lead has two bands which can be identified with  $\tilde{\sigma}_{111}$  and  $\tilde{\sigma}_{200}$ . In analogy with results obtained from the van Alphen–de Haas effect,<sup>[8]</sup> one can assume that the maximum of the  $\tilde{\sigma}_{111}$  band occurs at higher  $\omega$  than the  $\tilde{\sigma}_{200}$  maximum. Both bands superimpose at all temperatures. The bands were separated by the following method. The effect of the  $\tilde{\sigma}_{200}$  band on  $\tilde{\sigma}_{111}$  was neglected to a first approximation. Extrapolating linearly the steepest part of the long-wave edge of  $\sigma_{111}$  to zero,  $\tilde{\sigma}_{200} = \tilde{\sigma} - \tilde{\sigma}_{111}$  was determined in this approximation. The position of the maximum, its height, as well as the parameter  $\gamma'$  characterizing the spread of the energy levels were found by a method described in [3]. Further, in the next approximation we plotted the  $\omega$  dependence of  $\tilde{\sigma}_{200}$  in the region in which the bands superimposed according to the formula

$$\tilde{\sigma}_g = \text{const} \cdot I(\omega), \quad (7)$$

matching both the position and the value of the calculated and experimental maxima of  $\tilde{\sigma}_{200}$ . Here  $I(\omega)$  is a function introduced in [3]; we calculated it for the values of  $\gamma'$  which we found. We find in this approximation  $\tilde{\sigma}_{111} = \tilde{\sigma} - \tilde{\sigma}_{200}$ . The results of separating the bands are shown in Figs. 2–4 by the dashed line.

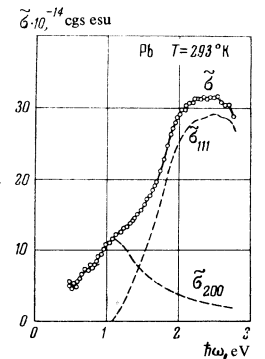


FIG. 2. The dependence of  $\tilde{\sigma}$  on  $\omega$  for  $T = 293^\circ \text{K}$ . Circles—experimental values of  $\tilde{\sigma}$ . The bands referring to  $\tilde{\sigma}_{111}$  and  $\tilde{\sigma}_{200}$  are marked by the dashed lines.

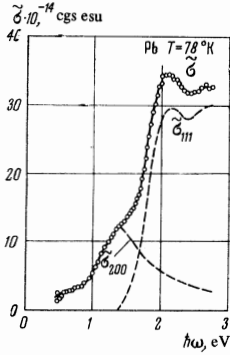


FIG. 3. The dependence of  $\tilde{\sigma}$  on  $\omega$  for  $T = 78^\circ\text{K}$ . Circles—experimental values of  $\tilde{\sigma}$ . The bands referring to  $\tilde{\sigma}_{111}$  and  $\tilde{\sigma}_{200}$  are marked by the dashed lines.

It should be noted that the results of the measurements at  $T = 78^\circ\text{K}$  carried out up to  $\hbar\omega \approx 2.8$  eV indicate the presence of structure in the  $\tilde{\sigma}_{111}$  maximum. It is apparently a double maximum. At room temperature this structure is very weakly exhibited. However, it reappeared systematically in all measurement series, and is therefore not an experimental error. At room temperature, too, the large width of the  $\tilde{\sigma}_{111}$  band indicates the presence of structure. No structure is visible at helium temperature, because the measurements were carried out only up to  $\hbar\omega \approx 2.15$  eV. Investigations of the structure of the  $\tilde{\sigma}_{111}$  maximum require detailed measurements in the near ultraviolet region. We assume that this structure is connected with the spin-orbit interaction which is rather strong in the case of lead.

3. The obtained results make it possible to determine the values of the Fourier components of the pseudopotential of lead by using the expression<sup>[3]</sup>

$$2|V_g| = \hbar\omega_{\max}/t. \quad (8)$$

Here  $t$  is a coefficient of the order of unity. Its value for various  $\gamma'$  has been calculated in<sup>[3]</sup>. The deviation of the coefficient  $t$  from unity for all  $\gamma'$  does not exceed 6 percent.

If the assumption about the spin-orbit splitting of the  $\tilde{\sigma}_{111}$  is correct, then one should substitute in (8), instead of  $\omega_{\max}$ , the value of  $\omega_0$  corresponding to the center of the band. At room temperature  $\omega_0 \approx \omega_{\max}$ , at nitrogen temperature one can expect that  $\omega_0$  coincides with the position of the local minimum between the two maxima. Unfortunately, the position of  $\omega_0$  at helium temperature can only be indicated approximately. Below we shall determine  $V_g$  both from  $\omega_0$  and from  $\omega_{1\max}$  corresponding to the left-hand maximum<sup>3)</sup>. The results of the determination of the Fourier components of the pseudopotential for lead are given in Table IV.

The values of  $\omega_{\max}$ ,  $\omega_0$ , and  $\omega_{1\max}$  were determined with an accuracy of 1–5 percent. This accuracy is related to the width of the maxima and their overlap. Changing the parameters of the conduction electrons within their error limits has practically no effect on the determination of the above frequencies. The error in the determination of  $V_{200}$  is also of the order of 1–5 percent. The error in  $V_{111}$ , connected with the error in  $\omega_{1\max}$  or  $\omega_0$ , amounts to about 1 percent. The differ-

<sup>3)</sup>The presence of some structure in the region of the  $\tilde{\sigma}_{111}$  maximum at room temperature makes it possible to determine  $\omega_{1\max}$  also at that temperature.

Table IV. Determination of the Fourier components of the pseudopotential for lead

$T, K$	{200}		{111}			
	$\omega_{\max}, \text{eV}$	$ V_g , \text{eV}$	$\omega_{1\max}, \text{eV}$	$\omega_0, \text{eV}$	$V_g, \text{eV}$	
					From $\omega_{1\max}$	From $\omega_0$
293	1.08	0.51	2.24	2.48	1.06	1.17
78	1.38	0.65	2.14	2.38	1.02	1.13
4.2	1.48	0.70	2.07		1.00	1.11*

\*This value of  $V_{111}$  was obtained using the value of  $V_{111} = 1.13$  referring to  $T = 78^\circ\text{K}$  with allowance for the temperature dependence of  $V_{111}$  determined from the preceding column.

ence between the two values of  $V_{111}$  obtained from  $\omega_{1\max}$  and  $\omega_0$  amounts to 10 percent.

4. One can compare the theoretical and experimental values of  $\tilde{\sigma}_g$  at the maximum. According to<sup>[3]</sup>

$$\tilde{\sigma}_g = \frac{1}{12} \frac{e^2}{\pi^2 \hbar^2} n_g p_g I. \quad (9)$$

Here  $e$  is the electron charge,  $p_g$  is the distance from the center of the Brillouin zone  $\Gamma$  to the Bragg plane with index  $g$  in momentum space,  $n_g$  is the number of physically equivalent planes  $g$ ,  $I$  is the same function of  $\omega/\omega_g$  and  $\gamma'$  as in (7) whose maximum values for various  $\gamma'$  have been calculated in<sup>[3]</sup>, and  $\omega_g = 2|V_g|/\hbar$ . For a face-centered cubic lattice  $n_{111} = 8$  and  $n_{200} = 6$ . The calculated and experimental values of  $\tilde{\sigma}_g$  are compared in Table V. The table also lists the  $\gamma'$  and  $p_g$  used in the calculation. In calculating the quantities  $p_g$  allowance was made for the temperature dependence of the lattice constant  $a$ . The value of  $\gamma'$  for the  $\tilde{\sigma}_{111}$  band was determined from the left-hand maximum.  $\gamma'$  was determined with an accuracy of 5–10 percent. The accuracy of the experimental determination of the maximum value of  $\tilde{\sigma}$  amounted to 2–5 percent. The accuracy of the calculated theoretical values of  $\tilde{\sigma}_{\max}$  was determined by the accuracy with which  $\gamma'$  was determined.

5. In addition to the conductivity maxima  $\tilde{\sigma}_{111}$  and  $\tilde{\sigma}_{200}$  described above, an additional small absorption is observed in lead in the region  $\lambda > 1.4 \mu$  (this can be seen from Figs. 2–4); the latter cannot be removed by any sensible change in the parameters referring to the conduction electrons. This absorption is observed at all temperatures. The ratio of the value of  $\tilde{\sigma}$  in this region (for  $\hbar\omega \approx 0.6$  eV) to the maximum value of  $\sigma$  is  $\sim 3$  percent at  $T = 4.2^\circ\text{K}$ ,  $\sim 8$  percent at  $T = 78^\circ\text{K}$ , and

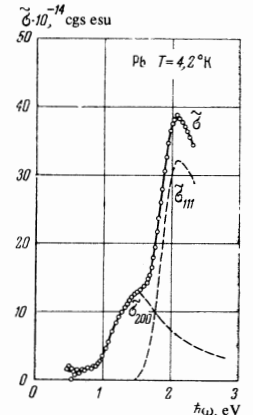


FIG. 4. The dependence of  $\tilde{\sigma}$  on  $\omega$  for  $T = 4.2^\circ\text{K}$ . Circles—experimental values of  $\tilde{\sigma}$ . The bands referring to  $\tilde{\sigma}_{111}$  and  $\tilde{\sigma}_{200}$  are marked by the dashed lines.

**Table V.** Comparison of the theoretical and experimental values of  $\tilde{\sigma}_g$  at the maximum

T, °K	{200}				{111}			
	$\gamma'$	$p_g \cdot 10^{10}$ , g-cm/sec	$\tilde{\sigma}_{max} \cdot 10^{-14}$ , cgs esu		$\gamma'$	$p_g \cdot 10^{10}$ , g-cm/sec	$\tilde{\sigma}_{max} \cdot 10^{-14}$ , cgs esu	
			exp	theor.			exp	theor.
293	0.27*	1.34	11.6	10	0.21	1.16	28.5	14
78	0.20	1.34 <sub>6</sub>	12.1	12	0.15	1.16 <sub>6</sub>	29.4	17
4.2	0.20	1.35	12.9	13	0.10	1.17	32.3	22

\*In determining  $\gamma'$  for the  $\tilde{\sigma}_{200}$  band we took no account of shift of the zero level due to the additional absorption indicated below. This shift could make the value of  $\gamma'$  at room temperature too low.

~20 percent at  $T = 293^\circ\text{K}$ . The absorption disappears in the region of 0.2–0.3 eV. The investigation of the  $\tilde{\sigma}(\omega)$  dependence near this threshold requires more detailed and accurate measurements of the optical constants in this region.

This additional absorption is, in our opinion, connected with the indirect transitions of electrons located close to the Fermi surface to the unfilled band in the region of the W point. The energy difference between the nearest unfilled band at the W point and the Fermi level is about 0.2–0.3 eV,<sup>[8-9]</sup> which agrees with the threshold of the additional absorption estimated from our experimental data. A further argument favoring this assumption is the strong temperature dependence of this absorption.

It follows from the work of Moss<sup>[10]</sup> that the absorption connected with indirect transitions should be proportional to

$$\eta = \frac{(\hbar\omega - \Delta E_m + k\Theta)^2}{e^{\Theta/T} - 1} + \frac{(\hbar\omega - \Delta E_m - k\Theta)^2}{1 - e^{-\Theta/T}}. \quad (10)$$

Here  $\Delta E_m$  is the minimum width of the forbidden band,  $k\Theta$  is the phonon energy, and  $\Theta$  is the Debye temperature. For  $\hbar\omega - \Delta E_m \gg k\Theta$ ,

$$\eta \propto \frac{1}{e^{\Theta/T} - 1} + \frac{1}{1 - e^{-\Theta/T}}. \quad (11)$$

For lead ( $\Theta = 86^\circ\text{K}$ ) the ratio of the values of this quantity at room, nitrogen, and helium temperatures is 7 : 2 : 1. The experimentally obtained values of  $\tilde{\sigma}$  at those temperatures in the region  $\hbar\omega > 0.9$  eV are in the ratio of 5 : 2 : 1 which is in good agreement with the theoretical estimate.

## DISCUSSION OF RESULTS

1. It follows from Table IV that  $|V_{200}|$  changes appreciably with temperature, decreasing with increasing temperature. It is difficult to make any statement about the temperature dependence of  $|V_{111}|$ ; this dependence is much weaker.

The results obtained by the optical method can be compared with the data of Anderson and Gold obtained from the van Alphen–de Haas effect,<sup>[8]</sup> and with the results of the calculation of Animalu and Heine.<sup>[11]</sup> Anderson and Gold found  $V_{111} = -1.14 \pm 0.03$  eV and  $V_{200} = -0.53 \pm 0.03$  eV. These data refer to the temperature range of 1–4.2°K. The calculation of Animalu and Heine<sup>[11]</sup> yields:  $V_{111} = -1.16 \pm 0.14$  eV and  $V_{200} = -0.44 \pm 0.14$  eV. A comparison reveals that for  $V_{111}$  all the results are in sufficiently good agreement. For  $V_{200}$  the agreement is worse. The difference exceeds the experimental errors.

2. A comparison of the absolute values of  $\tilde{\sigma}$  at the maximum of both bands has been carried out in Table V. The theoretical values have been obtained from (9), the experimentally obtained values of  $\gamma'$  being used in the calculation of I. These values also appear in Table V. It follows from Table V that there is good agreement of the theoretical and experimental results for the  $\tilde{\sigma}_{200}$  band.

For the  $\tilde{\sigma}_{111}$  band the theoretical values are approximately smaller by a factor of two than the experimental ones. Although this difference, too, is outside the limits of the experimental errors, it is appreciably smaller than the difference between experiment and the theory that starts from isolated critical points. According to Phillips<sup>[12]</sup> a calculation of the oscillator strengths in accordance with this theory yields values 5–10 times smaller than the experimental values.

A possible reason for the observed discrepancy for the  $\tilde{\sigma}_{111}$  band is the use of too high values of  $\gamma'$  in the calculations. The theory has been developed without allowance for the simultaneous action of several Fourier components of the pseudopotential. Allowance for this fact leads to a broadening of the  $\tilde{\sigma}_g(\omega)$  curve which is unrelated to the broadening  $\gamma'$  of the energy levels. Because of this the experimental values of  $\gamma'$  may turn out to be too high, a fact which will decrease the calculated values of  $\tilde{\sigma}_g$ .

Thus the agreement of the values of the Fourier components of the pseudopotential obtained by optical and other methods, as well as the agreement between the calculated and experimental values of  $\tilde{\sigma}$ , indicate that the interpretation of the observed bands is correct and confirm the additional possibilities of using metal optics to determine the Fourier components of the pseudopotential and their temperature dependence.

3. It follows from Table V that  $\gamma'$  is large at all temperatures. The spread of the energy level  $\gamma = 2\gamma'|V_g|$  amounts even at helium temperature to ~0.2 eV for the  $\tilde{\sigma}_{111}$  band and to ~0.3 eV for the  $\tilde{\sigma}_{200}$  band. The corresponding lifetimes  $\tau \lesssim 2 \times 10^{-15}$  sec are considerably less than the value  $\tau = 2.5 \times 10^{-14}$  sec obtained from results referring to the conduction electrons.

The possible reason for such small values of  $\tau$  are indicated in<sup>[13]</sup>. Here we would like to indicate in addition the possible influence of the collective Auger effect noted in<sup>[13]</sup>.

4. The Fourier components of the pseudopotential which have been obtained allow one to determine the concentration of the conduction electrons  $N_{\text{opt}}$  in accordance with formulas (10)–(11) of<sup>[1]</sup>. Inasmuch as we have obtained for  $V_{111}$  two values, determined from the center of the band (from  $\omega_0$ ) and from its left-hand edge (from  $\omega_{1,\text{max}}$ ), we obtain also two values of  $N_{\text{opt}}/N_a$  ( $N_a$  is the concentration of atoms). Table VI lists both of these values for all the three temperatures. The Table also lists values of  $N_{\text{opt}}/N_a$  obtained from the results of optical measurements in the long-wave region of the spectrum. It is seen from the table that at each temperature the three values of  $N_{\text{opt}}/N_a$  are in sufficiently good agreement. They are appreciably smaller than the value  $N_{\text{val}}/N_a = 4$ . Here  $N_{\text{val}}$  is the concentration of valence electrons. Particularly good is the agreement between the values obtained in the long-wave

**Table VI.** Electron characteristics of lead obtained by various methods

		$T = 293^\circ \text{ K}$	$T = 78^\circ \text{ K}$	$T = 4,2^\circ \text{ K}$
$N_{\text{opt}}/N_a$	From values of $V_g$ $\left\{ \begin{array}{l} \text{From } \omega_{1\text{max}} \\ \text{From } \omega_0 \end{array} \right.$	1,42	1,30	1,29
	From measurements in the long-wave region	1,25	1,13	1,13
		1,23	1,15	1,11
$S_F/S_F^0$	From formula (12) from [1]	0,62	0,61	0,61
	From (12) of this paper	0,56	0,53	0,53
$v_F/v_F^0$	From (13) of this paper	0,50	0,46	0,46
	From (12) of this paper	0,56	0,53	0,53
$S_F^0 \cdot 10^{21}, \text{ g}^2 \cdot \text{cm}^2/\text{sec}^2$		3,46	3,50	3,52
$v_F^0 \cdot 10^{-8}, \text{ cm/sec}$		1,82	1,83	1,84

region and those obtained from the center of the band. This is an additional confirmation of the fact that it is more correct to determine  $V_{111}$  from the center of the band.

We note that if use is made of the Fourier components of the pseudopotential obtained from the de Haas-van Alphen effect<sup>[8]</sup>, one finds  $N_{\text{opt}}/N_a = 1.34$  which is also in sufficiently good agreement with the value of this quantity obtained by other methods.

Thus, the difference between the concentration of conduction electrons and the concentration of valence electrons is basically determined by the Fourier components of the pseudopotential. The temperature dependence of  $N_{\text{opt}}$  is determined by the temperature dependence of the Fourier components of the pseudopotential<sup>[4]</sup>.

5. The obtained values of  $V_g$  make it possible to determine the total area of the Fermi surface  $S_F$  of lead, and the average velocity of the electrons on the Fermi surface  $v_F$ . The value of  $S_F/S_F^0$  was obtained both from the more exact formula (12) of<sup>[1]</sup>, as well as from the approximate formula<sup>[2]</sup>:

$$S_F/S_F^0 \approx v_F/v_F^0 \approx \sqrt{N_{\text{opt}}/N_{\text{val}}}. \quad (12)$$

The value of  $v_F/v_F^0$  was also determined according to two formulas: the more exact formula

$$v_F/v_F^0 = (N_{\text{opt}}/N_{\text{val}})(S_F^0/S_F) \quad (13)$$

and the approximate formula (12). These values are listed in Table VI. They have been calculated using the value of  $V_{111}$  obtained from the center of the band<sup>[5]</sup>. It is seen from Table VI that in the case of lead the values obtained from the approximate formulas differ from those obtained from the more exact formulas by about 10 percent.

The values of  $S_F$  and  $v_F$  obtained from the results of measurements in the short-wave spectral range practically coincide with those obtained from the results of measurements in the long-wave region. The use of potentials obtained by Anderson and Gold<sup>[8]</sup> yields

<sup>4</sup>If one makes use of the x-ray data on the temperature dependence of the diffraction peaks, then it is found that on going from room temperature to liquid nitrogen temperature  $N_{\text{opt}}$  decreases by 11 percent. [<sup>14</sup>] According to the data of Table VI, this decrease is 7 percent, which is in good agreement with the x-ray data.

<sup>5</sup>Use of the values of  $V_{111}$  found from the left maximum results in an increase of these values by about 4 percent.

$S_F/S_F^0 = 0.64$ , a value which is close to those cited in Table VI. An experimental determination of this value by means of the anomalous skin effect in the radio band<sup>[15]</sup> yields a value of  $0.55 \pm 0.05$ , which also agrees with the results presented in Table VI.

It is seen from Table VI that the Fermi surface of lead is considerably smaller than the Fermi surface of free electrons with a concentration equal to the valence concentration. The same applies to the mean velocity of the electrons on the Fermi surface.

In the last two columns of Table VI we cite values of  $S_F^0$  and  $v_F^0$  referring to free electrons with a concentration equal to the valence concentration. Use of these values in conjunction with the ratios  $S_F/S_F^0$  and  $v_F/v_F^0$  makes it possible to obtain values of  $S_F$  and  $v_F$  at all three temperatures. In calculating  $S_F^0$  and  $v_F^0$  account has been taken of the change of the lattice constant with temperature.

In conclusion we should note the considerable possibilities of metal optics which makes it possible to determine the fundamental characteristics pertaining to the conduction electrons, and their temperature dependence.

<sup>1</sup>R. N. Gurzhi and G. P. Motulevich, Zh. Eksp. Teor. Fiz. 51, 1220 (1966) [Sov. Phys.-JETP 24, 818 (1967)].

<sup>2</sup>A. I. Golovashkin, I. S. Levchenko, G. P. Motulevich, and A. A. Shubin, Zh. Eksp. Teor. Fiz. 51, 1622 (1966) [Sov. Phys.-JETP 24, 1093 (1967)].

<sup>3</sup>A. I. Golovashkin, A. I. Kopeliovich, and G. P. Motulevich, Zh. Eksp. Teor. Fiz. 53, No. 12 (1967) [Sov. Phys.-JETP, in press].

<sup>4</sup>A. I. Golovashkin and G. P. Motulevich, Zh. Eksp. Teor. Fiz. 44, 398 (1963) [Sov. Phys.-JETP 17, 271 (1963)]; A. I. Golovashkin, Zh. Eksp. Teor. Fiz. 48, 825 (1965) [Sov. Phys.-JETP 21, 548 (1965)].

<sup>5</sup>A. I. Golovashkin and G. P. Motulevich, Zh. Eksp. Teor. Fiz. 47, 64 (1964) [Sov. Phys.-JETP 20, 44 (1964)].

<sup>6</sup>G. P. Motulevich and A. A. Shubin, Optika i spektroskopiya 2, 633 (1957); A. I. Golovashkin, G. P. Motulevich, and A. A. Shubin, PTÉ No. 5, 74 (1960).

<sup>7</sup>G. K. White, Phil. Mag. 7, 271 (1962).

<sup>8</sup>J. R. Anderson and A. V. Gold, Phys. Rev. A139, 1459 (1965).

<sup>9</sup>T. L. Loucks, Phys. Rev. Letters 14, 1072 (1965).

<sup>10</sup>T. Moss, The Optical Properties of Semiconductors, Russ. transl. IIL, 1961.

<sup>11</sup>A. O. E. Animalu and V. Heine, Phil. Mag. 12, 1249 (1965).

<sup>12</sup>J. C. Phillips, Optical Properties and Electronic Structure of Metals and Alloys, Proc. International Colloquium, Paris, 1965, p. 22.

<sup>13</sup>P. Nozieres, Optical Properties and Electronic Structure of Metals and Alloys, Proc. International Colloquium, Paris, 1965, p. 363.

<sup>14</sup>G. P. Motulevich, Zh. Eksp. Teor. Fiz. 51, 1918 (1966) [Sov. Phys.-JETP 24, 1287 (1967)].

<sup>15</sup>J. E. Aubrey, Phil. Mag. 8, 1001 (1960).